22nd Australasian Fluid Mechanics Conference AFMC2020
Brisbane, Australia, 7-10 December 2020
https://doi.org/10.14264/fbfa901

Tidal Energy Feasibility Study and Turbine Design for Malolo Island

N. Joyce[1,2], A. Deo[2] and M. R. Ahmed[2]

[1]School of Science and Engineering

The University of the Sunshine Coast, Sippy Downs QLD 4556, Australia

[2]School of Engineering and Physics

The University of the South Pacific, Suva, Fiji

Abstract

Tidal current turbines have high potential for off-grid applications in Pacific Island nations due to the coastal proximity of the population. In this study, the feasibility of tidal current power extraction in a channel near Malolo Island, Fiji, was investigated. An Acoustic Doppler Current Profiler was used to collect 70 days of velocity data and the power density was estimated. Using a combination of Computational Fluid Dynamics and Blade Element Momentum theory, an array of bi-directional ducted horizontal axis tidal turbines was designed for the location. The analysis of the measured data indicated low power density; however, novel contributions were made, including quantification of the tidal resource at this previously unquantified site, design of a new hydrofoil with good hydrodynamic properties and optimised design of a constriction duct which significantly increased the power output.

Keywords

Tidal energy; Feasibility study; Hydrofoil; Turbine design; Annual energy production.

Introduction

Globally, there is a growing recognition of the need to transition from fossil fuels to renewable energy sources. Many Pacific Island countries consist of numerous small islands, many of which must establish mini-grids or 'off-grid' power systems to supply communities and small businesses with electricity. These remote locations often use generators which are reliant on imported fuel, or solar power. Amongst those currently relying on fossil fuels, there is an increasing desire to transition to renewable sources.

Small-scale solar and wind power systems have proven their effectiveness for off-grid applications and are a standard renewable solution for most remote areas. On the other hand, hydrokinetic tidal energy is a developing technology which is not as widely applied as solar and wind power due to the limited availability of suitable sites, detailed design requirements and high cost compared to established technologies where economies of scale have reduced the expense. Several grid-connected hydrokinetic tidal turbines have been successfully installed in the Northern hemisphere, although tidal energy's market share is still minimal compared to other renewable sources. Tidal current energy is a high-potential resource that should also be considered for Southern Hemisphere locations, and in particular it may be a suitable off-grid energy solution for remote coastal communities and businesses in the South Pacific.

For this study, the tidal resource in a natural channel near Malolo Island, Fiji, has been quantified and a feasibility assessment has been completed for a horizontal axis tidal current energy system in the channel. The island is located to the west of Fiji's main island, Viti Levu, and is a popular tourist destination.

Method

Several sites near Malolo Island were considered for detailed data collection. A Global Water Flow Probe (model FP111) was used to measure the tidal current speed at six different sites, and the site with the highest indicative current speed was selected. The chosen site has a depth of 24.3 m.

On the 11th of August 2019, an Acoustic Doppler Current Profiler (ADCP) was deployed by a diver at the bottom (seabed) of the channel. The average velocity over a 40 second period was measured every 10 minutes at 1 m vertical height intervals. In total, 70 days of velocity data were collected over a vertical range of 21 m.

The ADCP relies on an assumed salinity (on which the speed of sound depends) to calculate the velocity of the water. Since the salinity of the water was unknown at the time of deployment, an assumed salinity of 32 ppt was adopted. A sample of water was collected and tested to determine the true salinity and the speed of sound, c, was calculated using Mackenzie's equation (1) [9], which relates c to temperature, t (°C), depth, h (m), and salinity, s (%). The velocity data were then corrected using equation (2) [10].

$$c = 1448.96 + 4.591t - 5.304 \times 10^{-2}t^2 + 2.374 \times 10^{-4}t^3 + 1.340(s-35) + 1.630 \times 10^{-2}h + 1.675 \times 10^{-7}h^2 - 1.025 \times 10^{-2}t(S-35) - 7.139 \times 10^{-13}th^3 \quad (1)$$

$$v = v_{measured} \times \frac{c}{c_{assumed}} \quad (2)$$

The data were retrieved from the ADCP using Nortek's STORM software and a Weibull distribution was modelled to fit the velocity data using Justus' empirical method, which previous studies have shown to result in a close fit with minimal root mean square error and a good approximation of power density [1], [8]. The shape and scale factors were calculated using equations (3) and (4) respectively, where $\bar{v}$ is the mean velocity, σ is the standard deviation and Γ represents the gamma function.

$$k = \left(\frac{\sigma}{\bar{v}}\right)^{-1.086} \quad (3)$$

$$c = \frac{\bar{v}}{\Gamma\left(1+\frac{1}{k}\right)} \quad (4)$$

Eight constriction duct designs were modelled and tested using Ansys® Fluent, release 19.1, to determine the most efficient shape for increasing flow speed at the rotor. The duct which resulted in the greatest acceleration of the flow at the location

of the rotor from the CFD results was identified and the estimated acceleration due to the duct was then applied to the velocity data measured by the ADCP. New Weibull distribution parameters were then computed for a distribution that represented the constricted flow speed.

XFOIL, a program which uses panel method to calculate lift, drag and pressure coefficients around airfoils, was used to design a hydrofoil suitable for the site. Using the developed hydrofoil, an optimised turbine design was obtained using the genetic algorithm_based program Harp_Opt. The second Weibull distribution, representing the speed of the water at the rotor, was used to estimate the power output of this turbine.

Results

The peak velocity ranged from approximately 0.3 ms^{-1} during neap tides to 0.5 ms^{-1} during spring tides. The 70 day timeframe included 5 spring tides and 4 neap tides.

Figure 1 shows the direction of the current for speeds above 0.1 ms^{-1} for a cell height range of 2-15 m. The range 0-0.1 ms^{-1} has not been included in the graph as these slower currents act in many directions. Percentages displayed represent the proportion of time the current is flowing in a particular direction, separated into 1 degree segments. The ebb and flood currents act parallel and in opposite directions, which makes the location suitable for a bidirectional ducted turbine without the need for a yawing mechanism. The most frequent current directions are 78.5° from North and 259.5° from North.

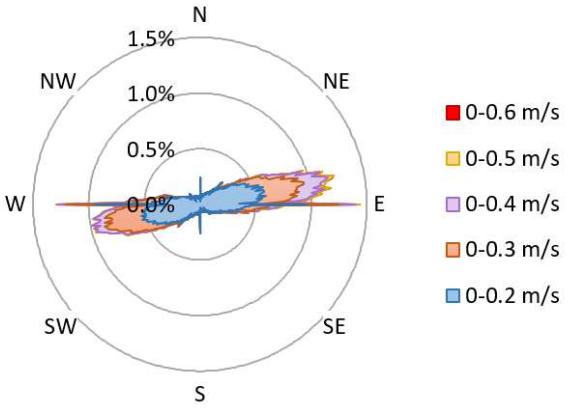

Figure 1. Velocity direction for different speeds at a cell height range of 2-15 m and a date range from the 16th of August until the 13th of October inclusive. Graph indicates that the flow reversal is parallel.

Figure 2 is a histogram of the average current speed at 10 minute intervals between 3 and 16 m from the ocean floor, which is the height range in which a tidal turbine would most likely be installed. The histogram uses two lunar cycles of data, from the full moon on the 16th of August 2019 to the full moon on the 14th of October 2019 (up to, but not including, this date). The highest current speed recorded was 0.706 ms^{-1}.

The power density of the resource was calculated using equation (5), the sum of the power density for each velocity multiplied by the probability of the velocity occurring. The power density for each speed was calculated using equation (6)

$$PD_w = \sum PD(v) \times f(v) \quad (5)$$

$$PD_w = \frac{1}{2}\rho V^3 \quad (6)$$

The power density for this resource is 4.247 W/m^2.

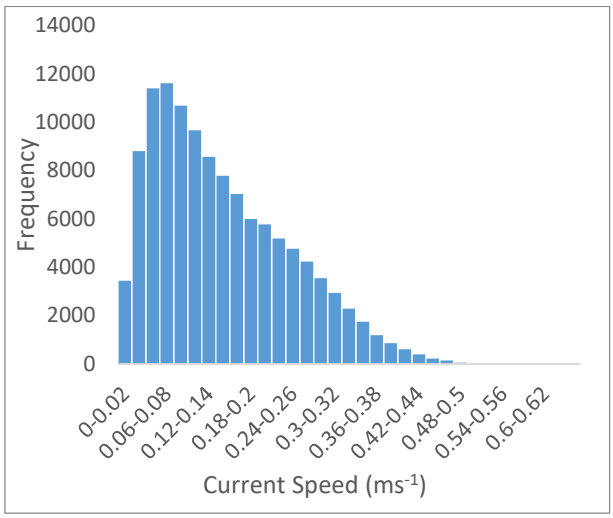

Figure 2. Histogram showing the frequency of speeds in 0.01 m intervals, over a cell height range of 2-15 m, equivalent to a height from the ocean floor of 3-16 m.

A Weibull distribution was made to fit the velocity data from the histogram in figure 2. A shape factor of 1.5904 and a scale factor of 0.16646 were calculated using equations (3) and (4). Equation (7) is the resulting probability density function.

$$f(v) = \frac{1.5904}{0.16646}\left(\frac{v}{0.16646}\right)^{0.5904} \exp\left(-\left(\frac{v}{0.16646}\right)^{1.5904}\right) \quad (7)$$

This Weibull probability density function is displayed in figure 3, with the probability of each speed occurring displayed on the left axis. The histogram is portrayed on the same graph to show the closeness of fit.

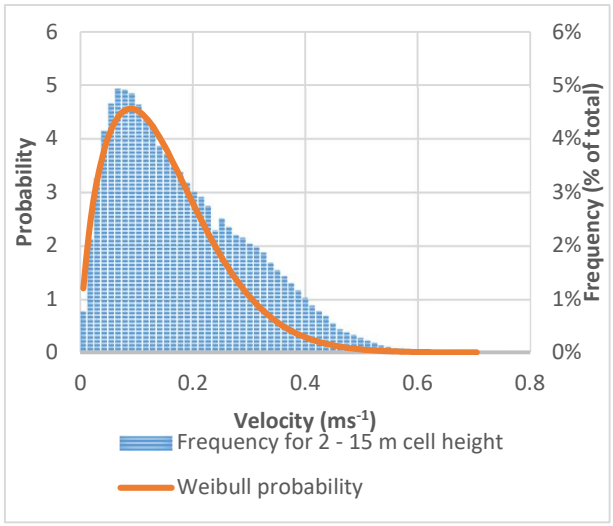

Figure 3. Weibull distribution with a shape factor of 1.5904 and a scale factor of 0.16646 fitted to the frequency data for current speed over a cell height range of 2-15 m. Probability values are given in the left hand column. The right hand column shows the percentage frequency of each bin of the histogram. The axes have been scaled by the inverse of the bin width to show an accurate comparison between the Weibull distribution and the histogram.

Discussion

Power density

The developed Weibull distribution is a good fit for the data as it provides an accurate approximation of power density. The percentage error of the Weibull power density compared to the true power density is 0.11%. However, this power density is low.

The power that may be harnessed by a turbine is proportional to the density of the water (ρ), the area of the turbine (A), the velocity of the water (V) cubed and the power coefficient of the turbine (C_p), as shown in equation (8) [4], [5].

$$P_t = \frac{1}{2}\rho A V^3 C_p \quad (8)$$

Of these, the variable with the greatest influence on the power produced is the velocity since it is cubed. Area and velocity are proportional according to the continuity equation (9).

$$A_1 V_1 = A_2 V_2 \quad (9)$$

Therefore, increasing the velocity by constricting the flow into a smaller cross-sectional area was expected to result in higher Annual Energy Production (AEP).

Maximum turbine dimensions

The channel is frequently trafficked by small vessels and occasionally by larger vessels, such as small cruise ships which may have a draft up to 4 m. Any HATCTs installed in this location must not interfere with the passing of these vessels. The lowest depth recorded for the site was 23.71 m during the spring tide on the 30th of August. Assuming a conservative minimum depth of 22 m, and allowing 6 m from the surface to the top of the turbine, the maximum height from the ocean floor that a turbine in this location may extend to is 16 m.

Since the water near to the ocean floor is turbulent, the bottom 3 m will also be excluded from the collection zone. This leaves the 3-16 m zone available for turbine deployment, which is equivalent to a cell height of 2-15 m relative to the ADCP. Therefore, a turbine in this location must not have a diameter greater than 13 m. To be conservative, the designed device is 10 m in diameter and its axis will be located 8 m from the ocean floor, resulting in an expected minimum distance of 9 m between the device and the surface of the water.

Turbine Design

Estimation of Acceleration due to Constrictor Duct

Due to the low speed of the tidal current, the power density of the site is small. However, the power density may be increased if a constriction duct is used.

CFD was used to estimate the acceleration that could be achieved with a bidirectional duct at this site. Eight constriction duct designs were tested which varied in inlet shape (circular or filleted square), closed and open exterior, linear or smooth contraction and incoming angle of the duct. It was found that circular ducts were more efficient than ducts with a filleted square inlet, even though the latter had a greater inlet area. Additionally, the smooth profile was more efficient than the linear profile. For ducts with the same inlet to rotor area ratio, increasing the length of the duct (reducing the incoming angle), resulted in higher velocities at the rotor. The smallest incoming angle tested was 10°, with smaller angles resulting in a duct of impractically long length.

The duct chosen for this design was the one which resulted in the greatest flow acceleration at the rotor. It had a circular area inlet 10 m in diameter and a rotor area 5 m in diameter. A velocity contour map of this duct is shown in Figure 4. A conservative inlet velocity of 0.2 ms^{-1} was used, resulting in a magnification factor of 3.096 at the rotor. An alternate test using an inlet speed of 0.5 ms^{-1}, representative of the maximum flow speed, resulted in a velocity magnification of 3.080. The multiplication factor of 3.080 estimated using CFD was applied to the velocity data collected from the channel at Malolo Island and new Weibull shape and scale factors of 1.5904 and 0.51269 respectively were determined to represent the speed of the constricted flow at the rotor.

The effectiveness of bidirectional ducts to accelerate flow through turbines has been well established through other studies [1], [3]. In the northern hemisphere, several ducted turbines designs have been installed in high-speed marine currents, although challenges such as economic viability have resulted in many ducted turbine companies reverting to 'bare' turbines of late [1].

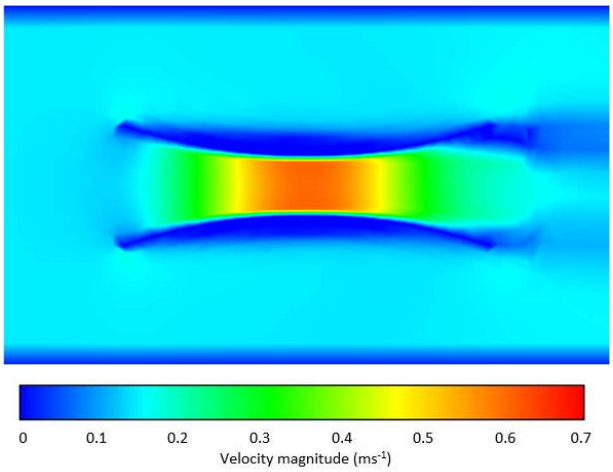

Figure 4. Velocity contours for the most effective shape tested, Duct 2. The constriction duct has a circular inlet with a diameter of 10m, an internal diameter of 5m and an inlet angle of 10°.

Design of Hydroturbine

A 7 bladed turbine with a TSR of 4 and a constant chord length was chosen for the analysis, based on values used in a previous study [7]. The diameter of the rotor area is 5 m.

One hydrofoil profile was chosen for the blade of the turbine. Since this is a ducted turbine, the tips are supported by the duct. Additionally, the blades will connect to a ring in the centre of the turbine which will provide additional support. This support means that reduction of the chord length and blade thickness will not be crucial for the design. To simplify the analysis, one profile with a thickness of 20% was chosen and is continuous throughout the blade. The chord length of 0.4 m was likewise kept constant; this chord length was chosen as it is the maximum allowable at the hub due to the number of blades.

The hydrofoil section design for this turbine was originally based on SG6043, an airfoil used for wind turbines. The new hydrofoil has a camber of 7 % and a leading edge radius of 1.19 % and maintains a good lift to drag ratio over a wide range of angles for low speeds, such as those encountered at the proposed location. The minimum cavitation number for this section, based on a maximum velocity of 1.5 ms^{-1}, was 11.5. The minimum coefficient of pressure for the section was investigated and it was determined that cavitation is unlikely to occur for angles of attack between -5° and 15°. The likelihood of cavitation is also reduced by the constriction duct, which reduces variations in angle of attack.

The lift and drag coefficients exported from XFOIL were extrapolated to cover 360° of angles of attack in QBlade using the Montgomerie method and were then input into Harp_opt for optimisation of twist angle and estimation of power output.

A variable speed fixed pitch turbine was chosen for the design and the rated power was set at 10 kW. A seed population of 100 was used for the optimisation and 50 generations were computed. The optimised twist angle distribution ranges from

37.38° in the centre of the turbine to 14.83° at the outer edge, as shown in figure 5, while figure 6 shows the final design of the ducted turbine and the constriction duct with dimensions.

Figure 5. 3D perspective view of the designed turbine blade showing the twist angle. The blade root is to the left and the tip is to the right.

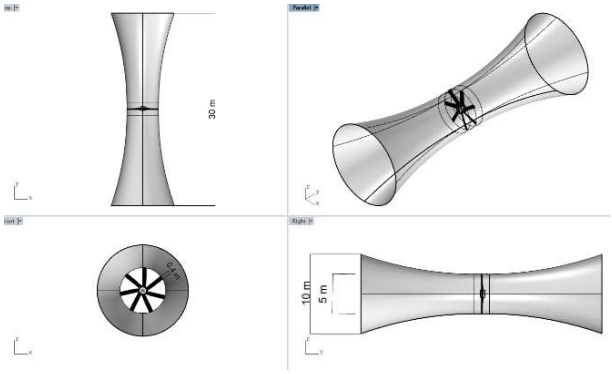

Figure 6. Drawings of the ducted turbine. The turbine has 7 blades and a diameter of 5m. The bidirectional duct has a diameter of 10m and an inlet angle of 10°.

Annual Energy Production

The rated power of the turbine is 10 kW, as increases in AEP were found to be very gradual for greater rated powers. A graph of the expected power output and power coefficient against flow speed is given in figure 7. Harp_Opt calculated that the AEP of this turbine is 9645.3 kWh per year.

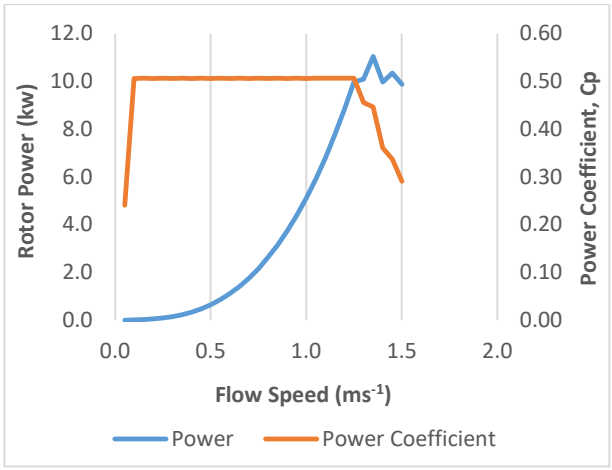

Figure 7. Rotor power (kW) and power coefficient, C_p, as a function of the flow velocity (ms^{-1})

For comparison, the same hydrofoil was used to estimate AEP for a bare turbine 10 m in diameter using the Weibull characteristics which represent the unconstricted flow. The AEP estimated by Harp_Opt for this bare turbine was 1455 kWh per year. Thus the AEP of the ducted turbine is anticipated to be 6.6 times greater than the AEP of a bare turbine of the same total device diameter. Despite this increase in AEP, the AEP of the ducted is low. For this reason, an array of 15 turbines across the channel at Malolo island can be installed that will produce at least 145 MWh per year. The true AEP is expected to be significantly higher due to the higher power coefficient resulting from blockage effect [6], which will cause the flow through the duct and the turbine to be at a higher speed.

Conclusion

The current speed data in a channel near Malolo Island was collected over a 70 day period and a ducted turbine designed. It is estimated that the AEP of a 15 turbine array proposed for the channel is at least 145 MWh. The anticipated increase in power output by a factor of 6.6 due to the constriction duct is significant, and indicates the need for future research in the area of cost effective manufacturing for ducted turbines and the development of new lightweight and corrosion resistant materials suitable for construction. The potential of tidal energy as an off-grid renewable solution for islands in the Pacific remains positive and more tidal energy feasibility studies should be conducted for other potential sites in the region.

Acknowledgments

The authors acknowledge and thank the staff of Malolo Island Resort and Subsurface Fiji for their assistance with this research.

References

[1] Belloni, C.S., Willden, R.H., and Houlsby, G. (2017). An investigation of ducted and open-centre tidal turbines employing CFD-embedded BEM. *Renewable Energy*, 108, 622–634, (DOI: 10.1016/j.renene.2016.10.048).

[2] Bilir, L., İmir, M., Devrim, Y., and Albostan, A. (2015). Seasonal and yearly wind speed distribution and wind power density analysis based on Weibull distribution function. *International Journal of Hydrogen Energy*, 40(44), 15301–15310, (DOI: 10.1016/j.ijhydene.2015.04.140).

[3] Borg, M.G, Xiao, Q., Allsop, S., Incecik, A., and Peyrard, C. (2020). A numerical performance analysis of a ducted, high-solidity tidal turbine, *Renewable Energy*, 159, 663–682, (DOI: 10.1016/j.renene.2020.04.005).

[4] Haas, K., Defne, Z., Yang, X., and Bruder, B. (2017). Hydrokinetic tidal energy resource assessments using numerical models. in Yang, Z. and Copping, A. (editors). *Marine Renewable Energy: Resource Characterisation and Physical Effects*, Springer, 99-120.

[5] Hu, Y. and Rao, S. (2011). Robust design of horizontal axis wind turbines using Taguchi method. *Journal of Mechanical Design*. 133(11), (DOI: 10.1115/1.4004989).

[6] Kim, K.P., Ahmed, M.R., and Lee, Y.H. (2012). Efficiency improvement of a tidal current turbine utilizing a larger area of channel. *Renewable Energy*, 48, 557-564.

[7] Laurens, J.M., Ait-Mohammed, M., and Tarfaoui, M. (2016). Design of bare and ducted axial marine current turbines. *Renewable Energy*, 89, 181–187, (DOI: 10.1016/j.renene.2015.11.075).

[8] Mohammadi, K., Alavi, O., Mostafaeipour, A., Goudarzi, N., and Jalilvand, M. (2016). Assessing different parameters estimation methods of Weibull distribution to compute wind power density. *Energy Conversion and Management*, 108, 322–335, (DOI: 10.1016/j.enconman.2015.11.015).

[9] National Physical Laboratory (2018). *Simple Equations*. viewed 24 December 2019. available at: http://resource.npl.co.uk/acoustics/techguides/soundseawater/content.html.

[10] Nortek AS (2008). *Aquadopp current profiler*. user guide. Nortek, Oslo.